Current Science International
ISSN: 2077-4435

Volume : 05 | Issue : 04 | Oct.- Dec. |2016
Pages**:** 481-496

Mineralogical Studies of Some Economic Minerals from El Burullus Lake Bottom Sediments

Anter F. Bkhit and Essam M. Esmail

Nuclear Materials Authority, Cairo, P.O.Box530, El-Maadi, Cairo ,Egypt

Received: 20 Oct. 2016 / Accepted: 30 November 2016 / Publication date: 10 December 2016

ABSTRACT

El Burullus area had several geomorphological units as the coastal sand dune, the coastal plain, the beach and cultivated lands. These sediments exhibit total heavy minerals content reach to 3.7 %. Moreover , they contain low radioactivity: eU (8ppm) and eTh (17ppm) indicating these sediments appear to be slightly favorable delivery sits for thorium but not for uranium which is probably due to the enrichment of thorium – bearing minerals as monazite mineral. Zircon is also recorded in these sediments. Furthermore, the study samples are potential sink for accessory minerals such as Fe,Ti minerals (magnetite, ilmenite, rutile and sphene) which represented 0.8 % ,1.3 % ,0.4 % and 0.02 % respectively. Also, garnet and cassiterite were recorded and displayed 3.0 % and 0.03 % respectively. In addition, it is clear that the concerned sediments exhibit enrichment of trace elements, as; Zr,Y,Nb,Ba,Sr,Zn and V. Zirconium is very considerably in their contents from 226 ppm to >10000 ppm. In row sand sample and concentrate sample respectively, is presumably due to the dominance of zircon mineral. Whereas the yettrium contents reach up to 3498 ppm especially in the concentrate sample. Meanwhile niobium content ranges from 10 ppm to 2050 ppm. Ba and Sr are more abundant in concentrate sediments than row sand samples; > 10000 and 3875 ppm respectively. Eventually V reaches up 3646 ppm. Also, a base metal (Cr) displays 2516 ppm. Consequently, it suggests that the concerned sediments may have been derived from various sources; acidic as well as basic rocks.

Key words: El Burullus area**,** geomorphological**,** sediments, heavy minerals

Introduction

El Burullus Lake is the most obvious geomorphic feature in the studied area. It is the second largest coastal lagoon after El-Manzala Lake.It locates at Lat. 31°30'N and long. 30° 50'E, in the coastal part of the north central Delta region Fig.(1a). El Burullus Lake has one out let which connects the Mediterranean Sea with the Lake at Burg El Burullus city as in Fig.(1b).It separated from the Mediterranean Sea along most of it length by a long sand dune bar where a relatively new international high way. El Burullus Lake covers currently a surface area of ~ 500km^2 (El-Reefy, 2006), Water depth 0.5 ~ 2m. It has a longitudinal shape nearly parallel to the shoreline and separated from the Mediterranean Sea by a narrow sand bar till Kom Mastarouh. Then, the coastal plain broadens to reach about 5 km at Sidi Youssef Village.With 55 km long and maximum width of 14 km. It is considered quite shallow with a maximum depth of about 2.5m (Kerambrum 1986).Although, various studies were conducted on the beach sediments as well as the sand dunes of the studied area e.g. Bakhit(1997), El Balakssy (2003), Omran E. Frihy and Khalid M. Dewidar (2003), Barakat (2004), Bakhit (2004), Hereher *et al*., (2011), Abeer A. El Saharty *et al*.,(2012) and Abdel Razek and Bakhit (2007) but the mineralogical studies of El Burullus Lake bottom are insufficient. The change in the lagoon surface area reveals a drastic shrinking during the 38 years of investigation. In 1973, the lagoon area was 430 km2 and in 1984 it was 385 km2. The lagoon area continued shrinking to 330 km2 in 1990, 280 km2 in 1999 and 260 km2 in 2005. Finally, the lagoon approached only 246 km2 in 2011 with a total loss of 184 km2 (42.8%) of its area between 1973 and 2011. It is obvious that the number and area of islands have also increased in the lake. (Hesham M. El-Asmar. *et al*., 2013) (Fig.4). Therefore, the aim of the present study is to investigate the mineralogical of El Burullus Lake bottom sediment to depth ranging from 5m to 8m during the cleaning and deeping the base of the Lake during season 2014.

Corresponding Author: Essam M. Esmail, Nuclear Materials Authority, Cairo, P.O.Box530, El-Maadi, Cairo, Egypt
E-mail: essam_12mem@yahoo.com

Sampling:

Ten samples weighting about 50 kg were taken at equal distance from the producing of Lake during the deeping and cleaning the lake to depth ranging from 2m to 7m (Fig.2); Illustrates the cleaning stages of El Burullus Lake, Also (Fig.3) illustrates the stages of the sample collection.

Methodology:

Two main types of technological composite sample as well as laboratory sample were taken. Flow sheet shows the treatment of technological and laboratory samples were shown in (Fig.5).The technological composite sample was taken along the accumulation of the producing sediment lake bottom. The concerned producing sediments were subjected to the separation using Wilfley Shakiing Table, (Fig.6), to obtain a sufficient concentrate of mineral varieties. These concentrate will be investigated under (ESEM) lab using (EDX) and (BSC) image, radiometric measurements, X-ray fluorescence (XRF) and X-ray diffraction (XRD). The sample separated to four parts: the first for grain size analysis for row sand and the concentrates Table (1), the second for heavy liquid separation while the third for radiometric measurements using gamma-ray spectrometry, the last one keeping as reference sample.

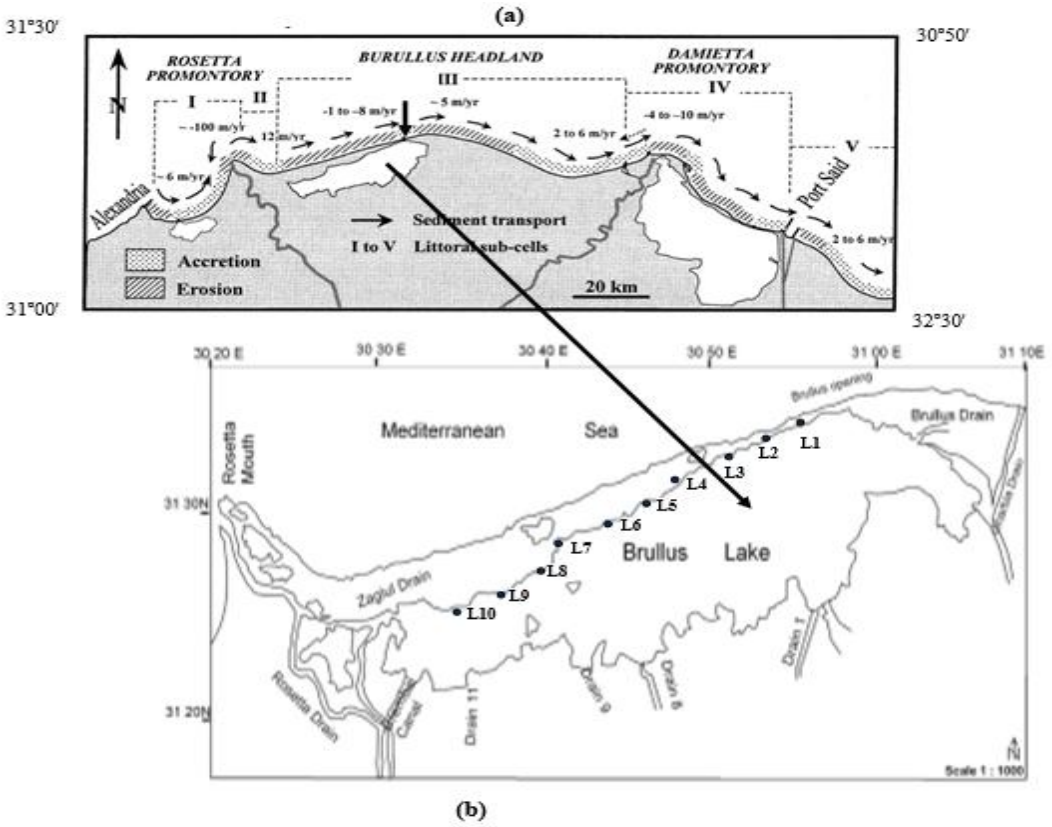

Fig. 1a and b: (a) Location map of El Burullus Lake. (After Frihy and Dewidar, 2003) (b) Sample location.

Table 1: Grain size analysis of sediment in El Burullus Lake bottom.

Sand size class (mm)	Row sand %	Concentrate %
+0.500 (coarse)	20.4	0.09
-0.500 + 0.250 (medium)	23.2	1.0
- 0.250 +0.125 (fine)	48.9	6.7
- 0.125 +0.075 (very fine)	4.5	79.3
-0.075 (silty size)	2.7	13.9

Fig. 2: Showing stages of deeping and cleaning of El Burullus lake.
(1) Dredging.
(2) Pipes connected by dredge push the bottom lake sediment out.
(3) Loader to accumulate sediment out on boundary of lake after drying.
(4) (a and b) Accumulation section of the lake bottom.
(5) Transportation of the lake sediment by cars.

Fig. 3: Stages of samples collections.
(1) Crushing from top to bottom.
(2, 3,4,5) Collecting of samples.
(6) The height of the production accumulation section.

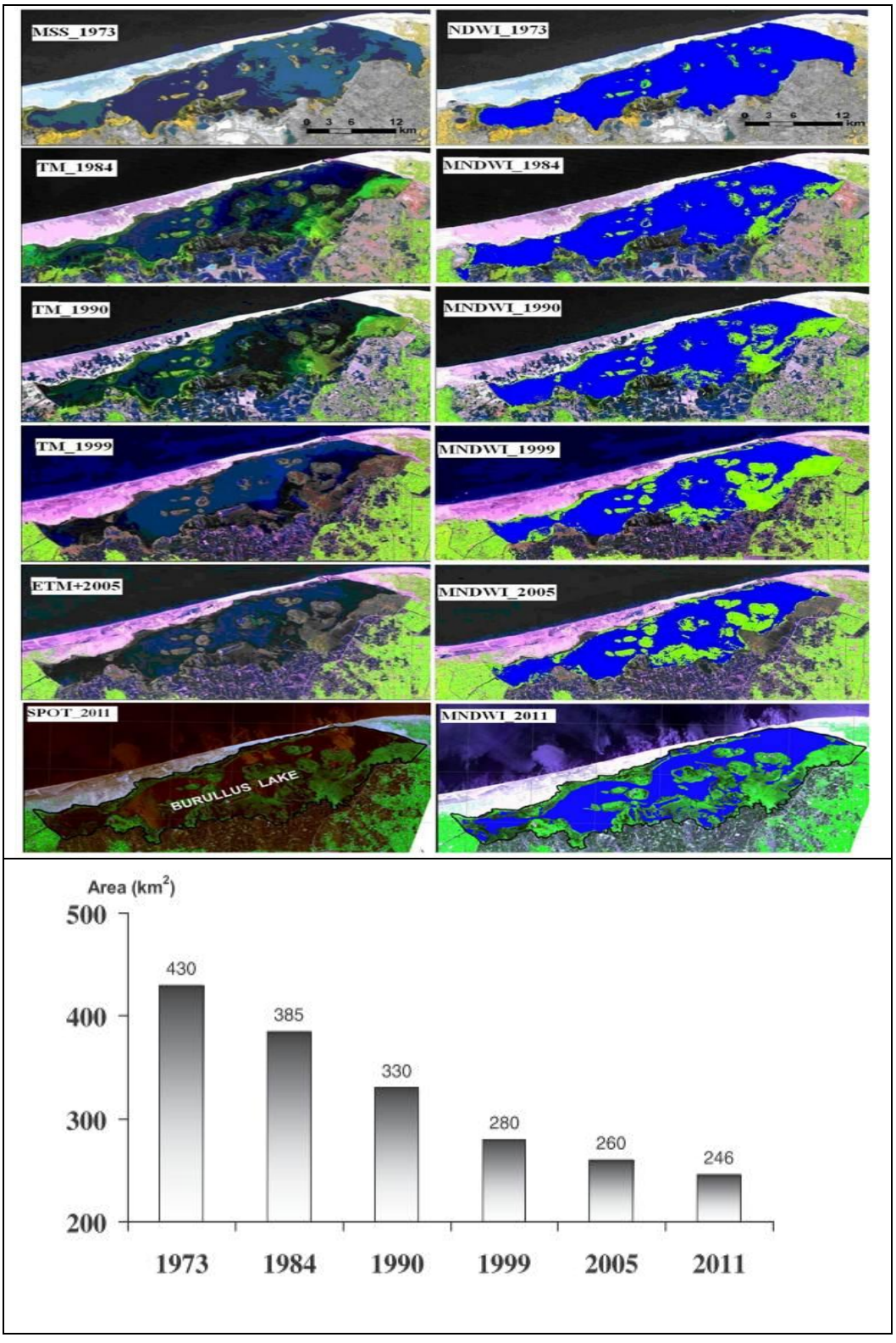

Fig. 4: Surface area change of the Lake El Burullus between 1973 and 2011. (After El Asmar, 2013).

Mineralogical Technique:

To identify the common heavy economic minerals constituent in the samples of in the studied area, selected samples were prepared for mineralogical study. These samples were quartered several times to obtain a representative sample of about 400 g. these samples were treated as follows: they stirred with water to get rid of the fine particles (silt -clay), also, using H2O2 to remove the organic materials as well as HCL to remove the iron oxides. The free sample was subjected to heavy liquid separation technique using bromoform liquid (sp.gr.2.85 g/cm3)

The heavy fractions were magnetically fractionated using a hand magnet to obtain the magnetite grains from the samples and; then the free-magnetite samples were magnetically fractionated using the Frantz Isodynamic Magnetic Separator (Model L1) at 0.2 amp., 0.5 amp., 1 amp., and 1.5 amp. The resulted magnetic sub-fractions were weighed and the frequency of each sub fraction was calculated .The heavy fractions were weighed and their percentages were calculated Table (2). A suitable content was taken from each magnetic sub fraction by quartering, and then counted under a binocular stereomicroscope. The weight percentage of the concerned heavy minerals was calculated according to Stakhov *et al*.,(1957) Table (3).The mineralogical investigation was achieved by ESEM and confirmed using X-ray diffraction technique(XRD) The recorded total heavy minerals are up to 3.7% Table (3).The microscopic study revealed that these minerals were arranged with descending order; ilmenite is main constituent in the studied samples, it represented by 1.3 %, follow by magnetite 0.8 %, zircon 0.7 %, garnet 0.5 %, rutile 0.4 %, cassiterite 0.03 %, sphene 0.03 % and monazite 0.01 %. On the other hand, both row sand samples and the concentrates were chemically analysis using XRF for trace elements measurements. The resulted data are shown in Table (4). From Table (4) it is clear that the concerned sediments exhibit enrichment of trace elements as: Zr, Y, Nb, Ba, Sr, Zn and V. Zirconium is very considerably in their contents from 226 ppm to > 10000 ppm, in row sand sample and concentrate sample respectively, is presumably due to the dominance of zircon minerals. Whereas the yettrium contents reach up to 3498 ppm especially in the concentrate sample. Meanwhile niobium content ranges from 10 ppm to 2050 ppm. Ba and Sr are more abundant in concentrate than row sand samples with > 10000 and 3875 ppm respectively. Eventually V reaches up 3646 ppm. Also; a base metal Cr displays 2516 ppm. Consequently, it suggested that the concerned sediments may have been derived from various source, acidic as well as basic rocks.

Table 2: Percentage of sample in magnetic susceptibility.

Amp	Magnetite	0.2	0.5	1.0	1.5	1.5 non
%	0.5	76.4	1.3	2.7	0.3	2.8

Table 3: Mineral distribution of sediment in El Burullus Lake bottom.

Mineral	Total heavy	Ilmenite	Magnetite	Zircon	Garnet	Rutile	Cassiterite	Sphene	Monazite
%	3.76	1.3	0.8	0.7	0.5	0.4	0.03	0.02	0.01

Table 4: XRF analysis for row sand and concentrate sample (ppm).

Element	Cr	Ni	Cu	Zn	Zr	Rb	Y	Ba	Pb	Sr	Ga	V	Nb
Row sand	92	26	70	42	226	21	17	128	17	29	N.d	67	10
Concentrate	37	9	59	97	558	155	43	122	37	69	N.d	42	24
	2516	29	N.d	112	>10000	N.d	3498	<10000	163	3875	3	3646	2050

Nd: not detected

On the other hand the radiometric measurements of these sediments were detected and listed in Table (5). The studied row sand samples and the concentrate of the sediments have a unimodal distribution with the modal class lies in the fine and very fine sand size classes respectively.

Table 5: Radiometric measurements of sediment in El Burullus Lake bottom.

Samples	eU (ppm)	eTh (ppm)	eR (ppm)	K %
Ranges	8	17	1.0	1.22

Table 6: The represented separation elements from represented samples in the studied area (%).

Element	In the original sample (%)	In the studied area (%)
Ilmenite	1.3	35.00
Magnetite	0.8	21.5
Zircon	1.7	18.9
Garnet	1.5	13.5
Rutile	1.3	8.00
Cassiterite	0.06	1.6
Sphene	0.03	1.8
Monazite	0.01	1.3

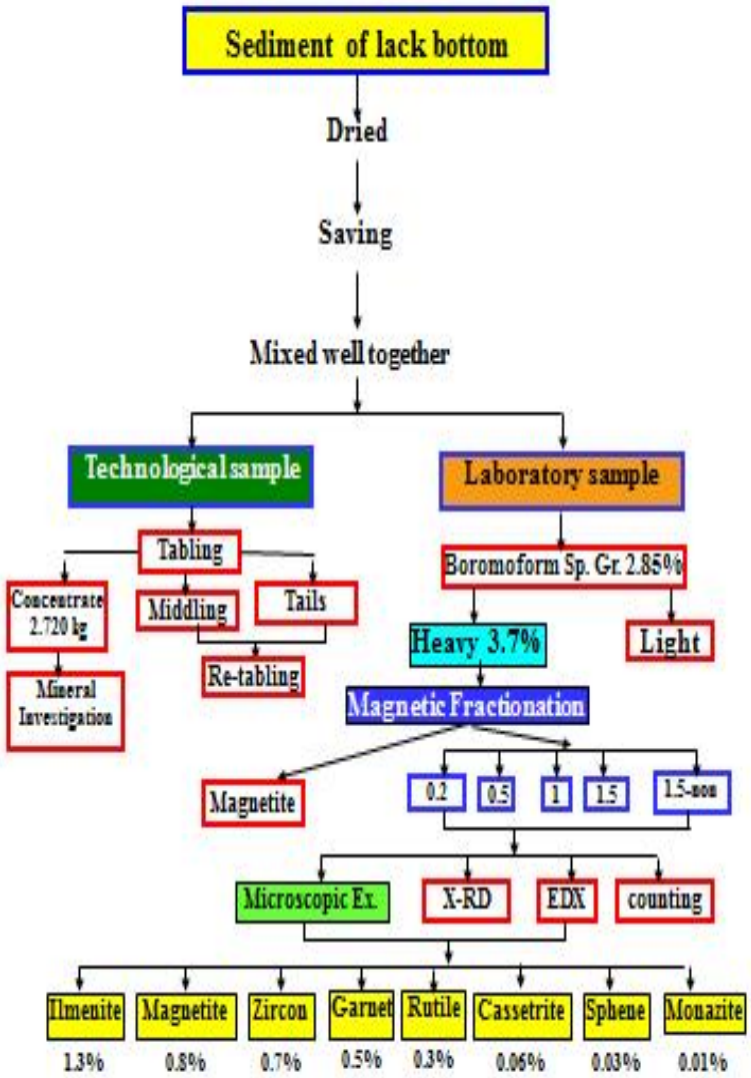

Fig. 5: Flow sheet illustrates the treatment of technological and laboratory samples.

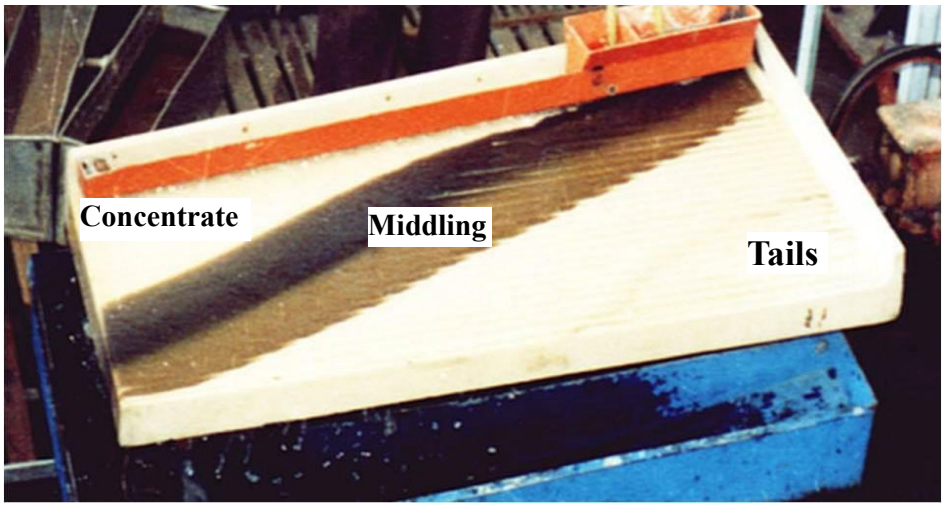

Fig. 6: Separation of product sediments using Wilfley shaking table.

The economic minerals in the studied area can be represented by: ilmenite, magnetite, zircon, garnet, rutile, cassiterite, sphene, monazite and titanium minerals. A brief description of these minerals as the following:

Ilmenite: FeTiO3:

Ilmenite represents the most frequent economic mineral in the studied samples. It is well rounded to sub-rounded black grains with its characteristic purple sub-metallic luster. The studied ilmenite represented 35 % in the studied area whereas it represented 1.3 % in the original sample, Table (6). In the boreholes, ilmenite is generally more or less similar in lateral distribution where it represents the major economic mineral (Fig.7) and Table (7).

Table 7: X-Ray diffraction pattern of ilmenite.

Sample		Ilmenite Astm card 3-0.81	
d/A^0	I/I_0	d/A^0	I/I_0
3.73	2	3.73	50
2.75	100	2.74	100
2.54	3	2.54	85
2.22	3	2.23	70
1.87	1	1.86	85
1.71	6	1.72	100
1.65	9	1.63	50
1.50	1	1.50	85
1.47	2	1.47	85

Magnetite: Fe3O4:

Magnetite is considered as one of the less stable minerals and can be altered to hematite, ulvospinel, magnetite and finally ilmenite. The Egyptian beach magnetite is characterized by its high content of titanium.The studied magnetite represented 21.5% in the studied area whereas it represented 0.8 % in the original sample Table (6). The presence of titanium in magnetite is attributed to the inclusion of titanium bearing minerals such as ilmenite or to the replacement of Ti^{4+} ion of 0.68A with Fe^{3+}/ of 0.64A in magnetite (Hammoud, 1966). The studied samples show high vanadium and titanium than the previous studies (El Balakssy, 2003), (Fig 8) and Table (8).

In boreholes magnetite content decreases with depth except in the most eastern borehole where the magnetite concentrations increase in the lower horizon. Generally, the vertical distribution of magnetite is similar to the distribution of total economic minerals.

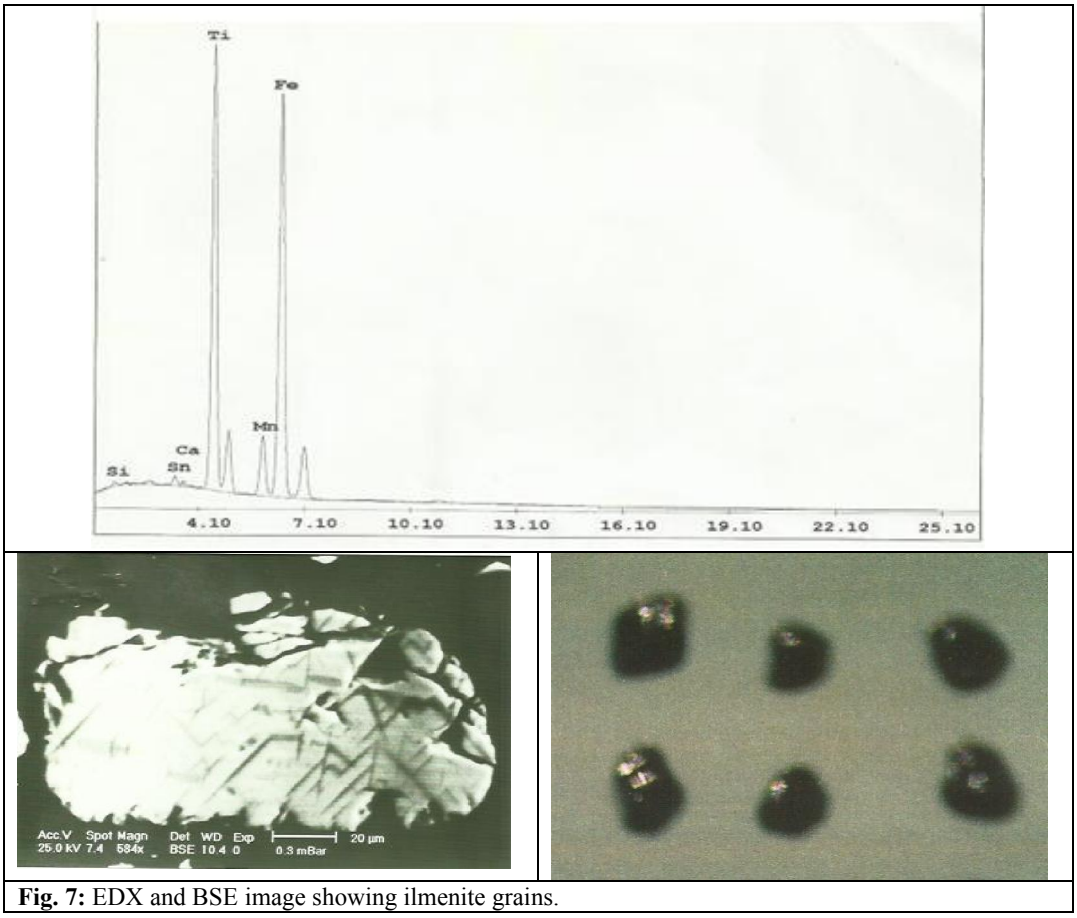

Fig. 7: EDX and BSE image showing ilmenite grains.

Table 8: X-ray diffraction pattern of magnetite

Sample		Magnetite Astm card (4-0551)	
d/A^0	I/I_0	d/A^0	I/I_0
4.85	7	4.85	8
3.70	4		
3.25	9		
2.97	31	2.97	30
2.74	11		
2.70	9		
2.53	100	2.53	100
2.42	5	2.42	8
2.22	2		
2.10	26	2.10	20
1.86	6		
1.72	11		
1.71	12	1.72	10
1.62	31	1.62	30
1.48	44	1.49	40

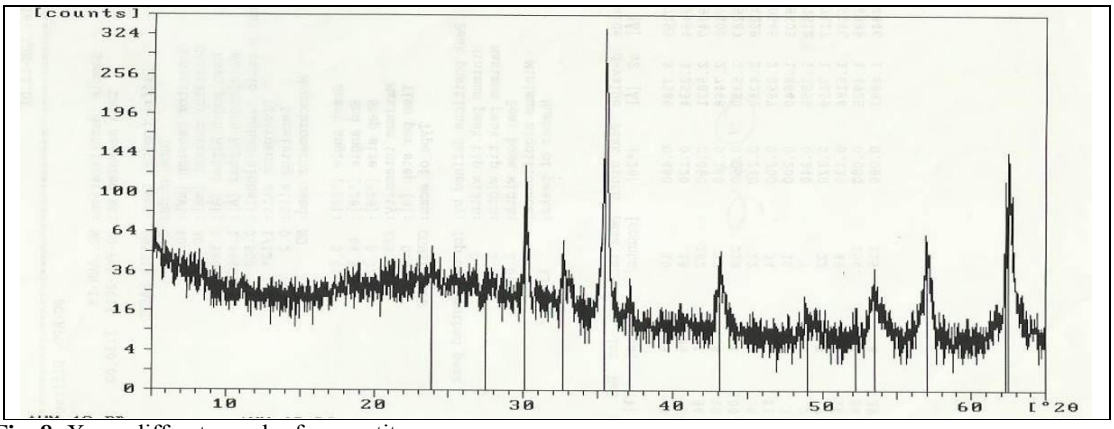

Fig. 8: X-ray diffractograph of magnetite.

Zircon: ZrSiO4:

The studied zircon represented 18.9 % in the studied area whereas it represented 1.7 % in the original sample, Table (6). Its particles are mainly water clear colorless but particles with pale shades of yellow, purple, honey, pink, cloudy and smoky are rare. Their particles are tetragonal prismatic bi pyramidal in shape (Fig. 9) and Table (9).

Table 9: X-Ray diffraction pattern of zircon.

Sample		Zircon Astm card (6-0266)	
d/A^0	I/I_0	d/A^0	I/I_0
4.44	12	4.43	45
3.3	100	3.30	100
2.52	9	2.518	45
2.34	2	2.336	10
2.22	3	2.217	8
2.06	3	2.066	20
1.91	0.3	1.908	14
1.75	1	1.751	12
1.71	6	1.712	40
1.65	9	1.651	14
1.55	0.3	1.547	4
1.50	1	1.495	4
1.48	3	1.477	8
1.38	0.3	1.381	10
1.36	1	1.362	8

.

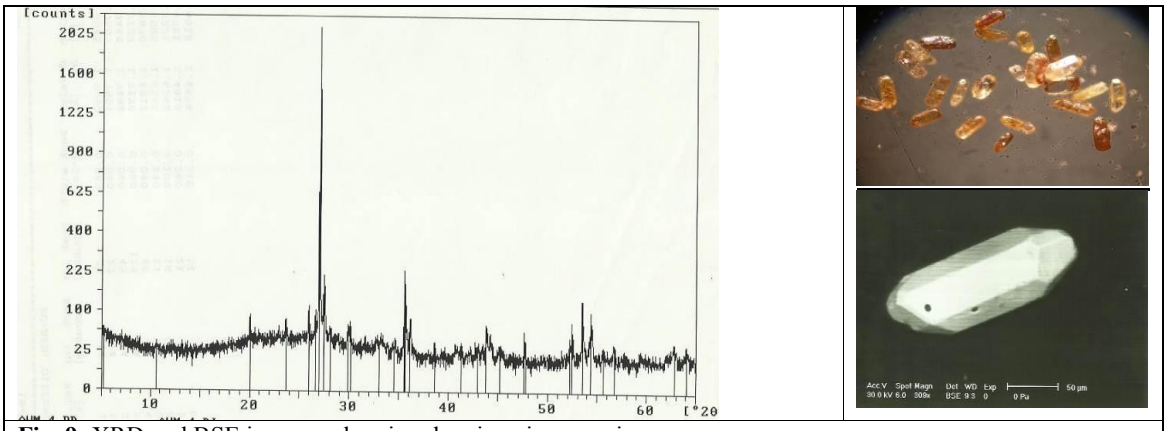

Fig. 9: XRD and BSE image and grains showing zircon grain.

Garnet: (Mg Mn Fe Cr Ti Ca Al) SiO4:

Garnet crystals are pale pink and colorless varieties. These varieties are the more abundant and belong to the almandine-pyrope species. Their sizes are relatively coarse and mainly coarser than 0.25 mm in diameter. Garnet has moderate magnetic susceptibility which varies slightly due to the variations in its chemical composition (El Balakssy, 2003).From Table (6) the studied garnet represented 13.5 % in the studied area whereas it represented 1.5% in the original sample (Fig.10)and Table (10).

Table 10: X-Ray diffraction pattern of garnet.

Sample		garnet Astm card (9-427)	
d/A^0	I/I_0	d/A^0	I/I_0
4.09	2	4.04	30
2.89	41	2.87	40
2.59	100	2.57	100
2.46	8	2.45	5
2.35	10	2.35	20
2.27	12	2.26	20
2.11	15	2.10	20
2.04	2	2.04	10
1.88	25	1.87	30
1.67	8	1.66	30
1.60	36	1.60	40
1.54	17	1.54	50

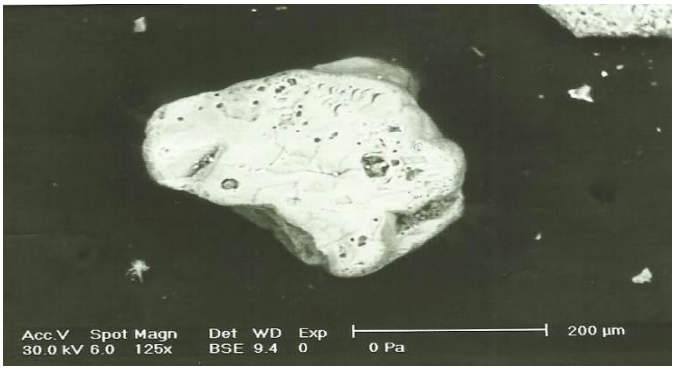

Fig. 10: BSE image showing garnet grain.

Rutile: TiO2:

Rutile is one of the most stable detrital minerals in sedimentary rocks. It is known that rutile may contain highly charged elements such as Nb, Cr, Fe, Al, Ni, Sb, Sn, Ta and W (Deer, 1962). The studied rutile represented 8% in the studied area whereas it represented 1.3 % in the original sample Table (6). Most of rutile grains are concentrated in very fine sand size (Dabbour, 1997 and Ibrahim, 1995). It is present as euhedral to subhedral grains with color varies from black, brown, red, orange to yellow. Rutile recorded in all studied samples with wide range of magnetic susceptibility. It shows general decrease of content with the depth (Fig.11) and Table (11).

Cassiterite: SnO2:

The studied cassiterite represented 1.6 % in the studied area whereas it represented 0.06 % in the original sample Table (6). It characterized by rounded grains and exhibits reddish brown color (Fig.12).

Table 11: X-Ray diffraction pattern of rutile.

Sample		Rutile Astm card 21-1276	
d/A^0	I/I_0	d/A^0	I/I_0
3.25	100	3.25	100
2.49	1	2.487	50
2.30	3	2.295	8
2.19	1	2.188	25
2.06	3	2.054	10
1.69	2	1.6874	60
1.62	3	1.6237	20
1.47	2	1.4797	10
1.45	3	1.4528	10
1.36	1	1.3598	20

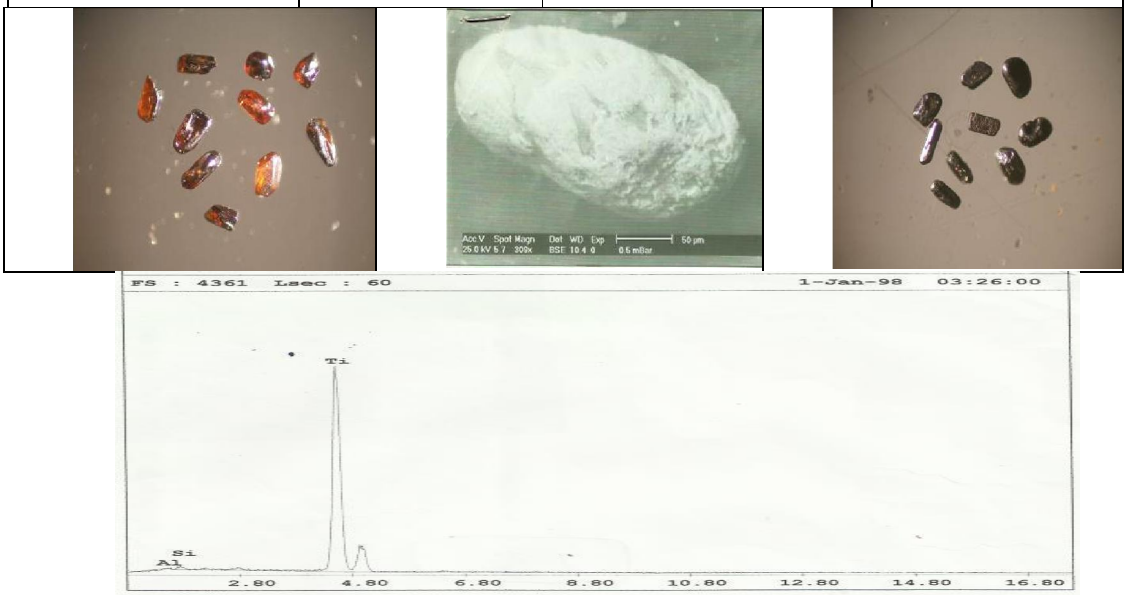

Fig. 11: EDX, and BSE image showing rutile grains.

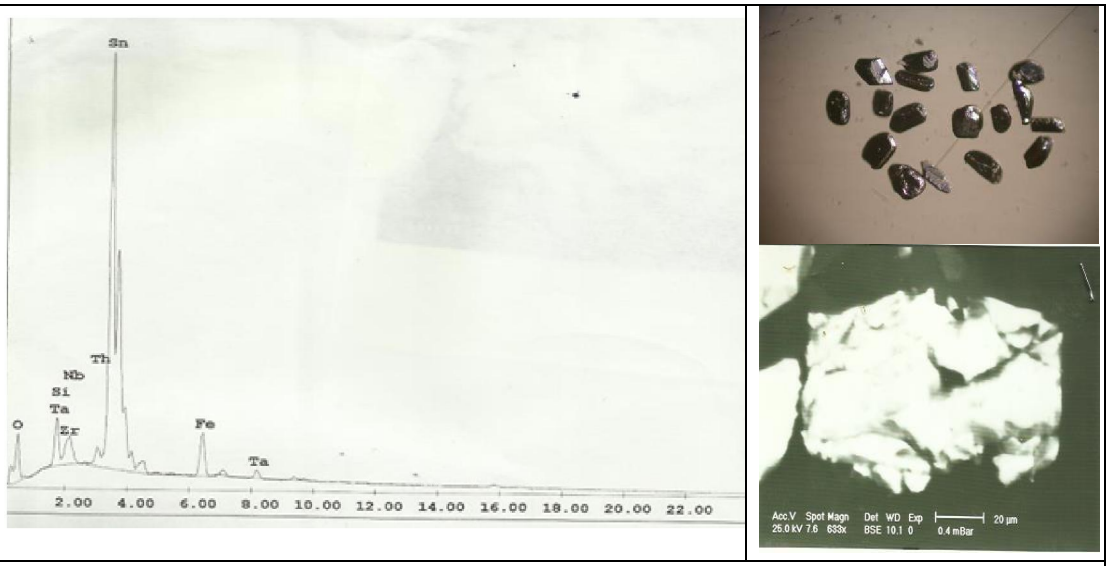

Fig. 12: EDX and BSE image showing casstrite grains.

Sphene: Ca Ti SiO4:

Sphene was fairly recorded in the present samples.The studied sphene represented 1.8 % in the studied area whereas it represented 0.03 % in the original sample Table (6). It displays subrounded particles with heavy lemon yellow color (Fig.13) and Table (12).

Table 12: X-Ray diffraction pattern of sphene.

Sample		Sphene Astm card 25-0177	
d/A^0	I/I_0	d/A^0	I/I_0
4.92	6	4.95	11
3.24	100	3.24	100
2.99	14	2.996	30
2.60	11	2.612	30
2.23	6	2.230	4
2.10	4	2.108	5
2.06	3	0.064	13
1.92	13	1.949	2
1.64	6	1.647	8
1.62	19	1.614	2
1.48	4	1.496	10
1.45	2	1.421	9

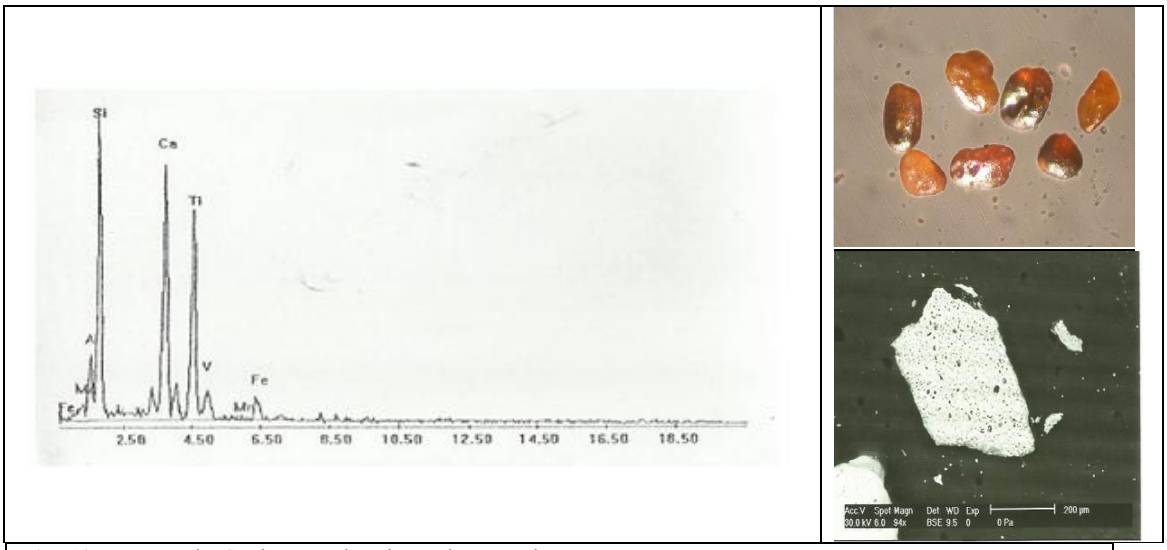

Fig. 13: EDX and BSE image showing sphene grains.

Monazite: (Ce La Th) PO_4:

The studied monazite represented 1.3 % in the studied area whereas it represented 0.01 % in the original sample, Table (6). Monazite is phosphate mineral which attains special importance source of rare elements such as thorium and REE; especially lanthanum, and cerium while uranium is present in small amounts. Monazite grains in the sediments are colorless with some tint of lemon yellow, honey yellow. Their grains are well rounded mostly oval in shape and free from inclusions. It is rare in the area it does not exceed 0.1% by ratio 0.3 % (Fig.14) and Table (13).

Table 13: X-Ray diffraction pattern of monazite.

Sample No.		monazite (11-556)	
d/A^0	I/I_0	d/A^0	I/I_0
5.2	4	5.20	13
4.80	9	4.82	7
9.69	10	4.66	18
4.19	21	4.17	25
4.10	8	4.08	9
3.50	46	3.51	25
3.31	57	3.30	50
3.10	100	3.09	100
2.99	14	2.99	18
2.87	47	2.87	70
2.61	6	2.61	18
2.45	6	2.44	18
2.41	5	2.40	5
2.34	2	2.34	5
2.19	14	2.19	18
2.15	12	2.15	25
2.13	16	2.13	25
1.97	12	1.96	25
1.90	5	1.90	13
1.87	17	1.86	18
1.80	4	1.80	9
1.77	8	1.76	18

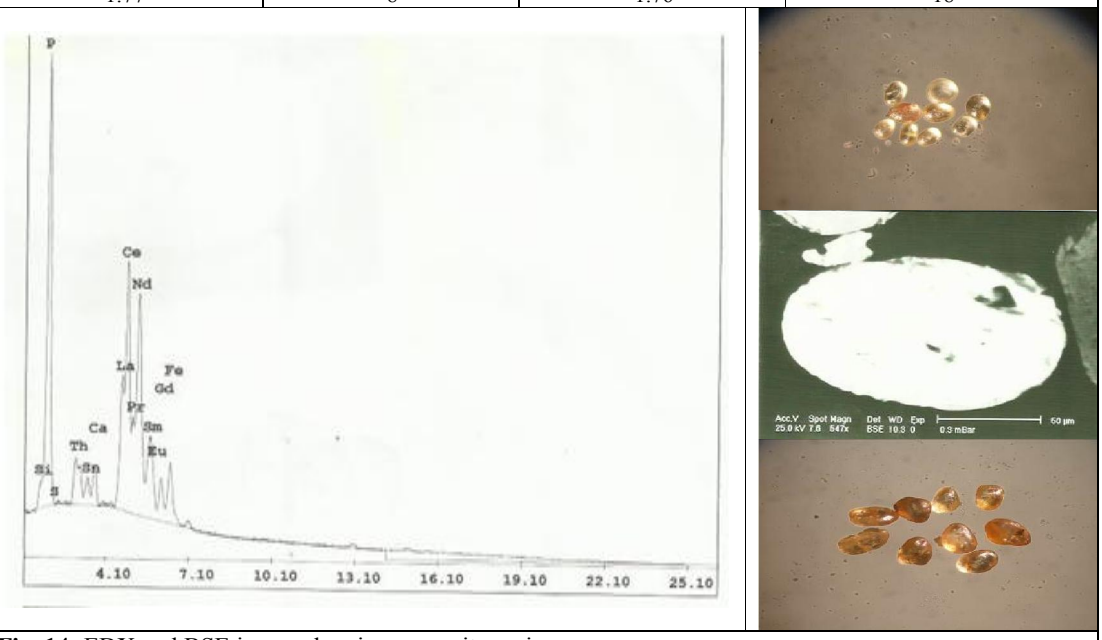

Fig. 14: EDX and BSE image showing monazite grains.

Titanium Minerals:

Titanium minerals in the study area are shown in table (14).

Table 14: EDX analysis data of titanium minerals.

Elements	Titano Magnetite	Ilmenite	Rutile	Sphene
Al2O3	1.08	3.21	0.97	-
SiO2	2.5	2.03	0.55	47.00
CaO	0.04	Nd	Nd	28.00
TiO2	14.60	45.50	95.43	35.00
MnO	0.89	0.55	Nd	-
FeO	92.00	45.97	2.73	-

Nd: not detected

Results and Discussion

El Burullus area had several geomorphological units as the coastal sand dune, the coastal plain, the beach and cultivated lands. The clay content and shells fragments represent more than 25 % from original sample during wishing process. The majority of heavy fraction lies in 0.2 % in magnetic fractionation by 76.4 % from heavy fraction. The studied row sand samples and the concentrate of the sediments have a unimodal distribution with the modal class lies in the fine and very fine sand size classes respectively. These sediments exhibit total heavy minerals content reach to 3.7 %. Moreover, they contain low radioactivity; eU (8ppm) and eTh (17 ppm) indicating these sediments appear to be slightly favorable delivery sits for thorium but not for uranium which is probably due to the enrichment of thorium – bearing minerals; monazite mineral. Furthermore, the study samples are potential sink for accessory minerals such as: Fe, Ti minerals, ilmenite, magnetite, rutile and sphene which represented 1.3 %, 0.8 %, 0.4 % and 0.02 % respectively. Also, garnet and cassiterite were recorded and displayed 3.0 % and 0.03 % respectively. In addition, it is shown that concentrate samples have the highest concentrations of Cr (2516 ppm), Zr (>10000), Y (3498), Ba (>10000 ppm), Pb (163), Sr (3875), V (3646) and Ub (2050 ppm). The majority of sample lies in very fine class by 79.3 % during the sieving of concentrate of sample flowed by silty size by 12.9 %, but in row sand or original sample the majority lies in fine class by 48.9 % flowed by medium class by 23.2 % . In addition to the present study shown the Lake Burullus is under the direct threat of environmental degradation due to the continuous human-induced shrinking. Another threat arises from the removal of the coastal sand dunes bordering its coastal face. This delicate coastal ecosystem requires appropriate management and protection as the country is moving toward sustainable use of its natural recourses.

References

Abdel-Razek,Y.A.and A.F. Bakhit, 2007. Comparison between the measurements of Radon Gas concentration and X-ray intensities on exploring the black sand El Burullus Beach: Arab Jour.Nuc1.Sci. App1.41: 4.

Abeer, A., El Saharty. *et al*., 2012. The radiological hazards of some radionuclides in Mariout and Brullus Lakes, Egypt. J. Rad. Res. Appl. Sci., 5: 2.

Bakhit, A.F., 1997. Evaluation of economic placer deposits on the drainage source area of the River Nile basin, M.Sc. Thesis, Institute of African studies, Cairo University, Cairo, p. .

Bakhit, A.F., 2004. Mineralogy and concentration of Heavy Economic Minerals Northern Delta, Ph.D. Thesis, Institute of African studies, Cairo University, Cairo, p.

Barakat, M.G., 2004. Sedimentological studies and evaluation of some black sand deposits on the Northern coast of Egypt, M.Sc. Geol. Faculty of Science, Alexandria University, Alexandria, p.

Dear, A.O., 1992. An introduction to the rock forming minerals. The English Language Society and Longman, London.

Dabour, G.A., 1997. Mineralogical study on the opaque minerals and secondary rutile from the Egyptian black sands proceed. Egypt, Acad. Sci, 47: 105-121.

El Balakssy, S.S., 2003. Mineralogical studies for the economic minerals in the sand dunes belt at Baltim area, Egypt. Ph.D. Thesis, Fac. Sci., Ain Shams University, Cairo, p: 205.

El-Reefy, H.I, *et al*., 2006. Distribution of gamma-ray emitting radionuclides in the environment of El Burullus Lake soil and vegetations. Journal of Environmental Radioactivity, 87: 148-169.

Hammoud, N.M.S., 1966. Concentration of monazite from Egyptian black sands employing industrial techniques. M.Sc. Thesis, Fac. Sci., Cairo University, Cairo, p.

Hesham M. El-Asmar. *et al*., 2013. Surface area change detection of the Burullus Lagoon, North of the Nile Delta, Egypt, using water indices: A remote sensing approach, Egyptian Journal of Remote Sensing and Space Sciences, 16: 119-123.

Hereher, M.E., M.I. Salem and D.H. Darwish, 2011. Mapping water quality of Brullus Lagoon using remote sensing and geographic information system. Journal of American Science, 7(1): 138-143.

Ibrahim, 1995. Investigations of some physical properties of zircon and rutile to prepare high purity minerals concentrates from black sand deposited, Rosetta, Egypt. MSc. Thesis Fac. Sci., Mansoura University, El Mansoura, p.

Kerembron, P., 1986. coastal lagoons along the southern Mediterranean coast, Morocco and Tunisia: description and bibliography. UNESCO Rep. Mar.sci.,paris, 034: 184.

Omran, E., Frihy and Khalid M. Dewidar, 2003. Patterns of erosion/sedimentation, heavy mineral concentration and grain size to interpret boundaries of littoral sub-cells of the Nile Delta, Egypt. Marine Geology, 199: 27-43.

Stakhov, N.M., G.I. Bushinskii and I.V. Pustovalov, 1957. Metodyizocheniya ocadochnykh porod, torn. Methods of studying sedimentary rocks, V.1, Moskva Gosgeoitekhiz dat, p: 611.